

# The Shape of the Edge of a Leaf

M. Marder

Center for Nonlinear Dynamics and Department of Physics  
 The University of Texas at Austin, Austin TX 78712  
 marder@chaos.ph.utexas.edu

Leaves and flowers frequently have a characteristic rippling pattern at their edges. Recent experiments found similar patterns in torn plastic. These patterns can be reproduced by imposing metrics upon thin sheets. The goal of this paper is to discuss a case where the shape of a distorted and buckled sheet can be calculated analytically. In addition, a method to provide careful comparison between analytical solutions and direct numerical studies is presented. Approximate properties of composite buckling structures are presented in closing.

PACS numbers: 45.70.Qj,02.40.-k

## I. INTRODUCTION

A characteristic rippled pattern often appears at the edges of leaves and flowers. One can even produce it by ripping in half a thin sheet of plastic, such as a plastic bag[1]. A numerical example of a stretched sheet with two generations of waves appears in Figure 1. I have found a case where the mathematics of this problem can be solved exactly.

This topic touches on an interesting basic question, which concerns the complexity of the instructions needed to generate complex natural patterns. The dominant belief among biologists is that the curling shapes of plants are produced by detailed genetic instructions telling various sections to curl up and down[2]. The physics community interested in studying patterns would prefer to assume that complex forms are produced when possible by simple rules, a view with some support also among biologists[3, 4]. It is natural to guess that by imposing non-flat metrics upon thin sheets, elasticity alone will compel them to curl spontaneously into fractal forms. However, to proceed from a guess to a detailed demonstration requires some effort. Nechaev and Voituriez[5] have carried out the only other study along these lines of which I am aware, using conformal mapping techniques to analyze an exponentially growing metric, and it is nicely complementary to the work presented here.

I begin with a brief discussion of results from differential geometry that pertain to the shapes of flowers. I then proceed to a particular case where the equations for the edge of a leaf can be solved exactly, and its shape described in terms of elementary functions. Finally, I present evidence that although this exact solution is a local energy minimum, there are lower-energy structures for very long systems that have a more complicated hierarchical structure.

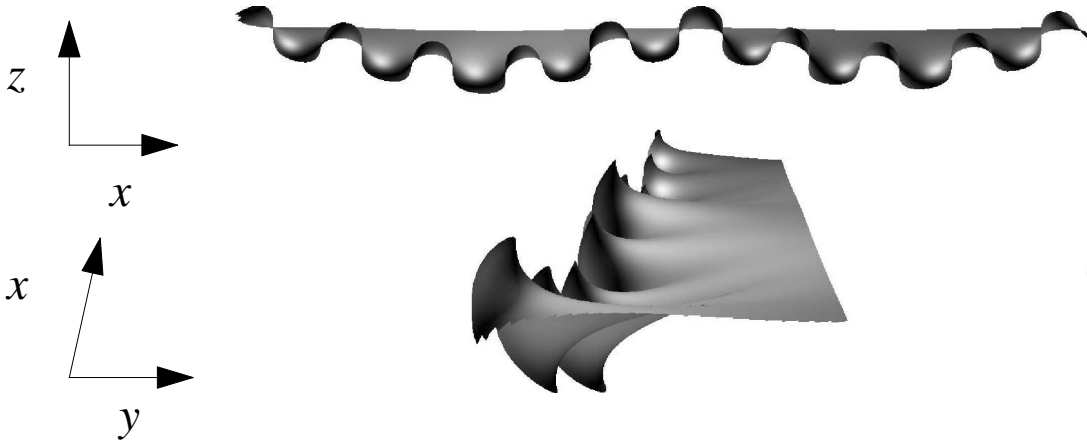


FIG. 1: Illustration of shapes produced by stretching a membrane at one end. This figure was produced by numerical minimization of Eq. 10 with  $\sqrt{g_{xx}(y)} = .7 \exp(-y/12) + .3 \exp(-y/36)$ . The numerical sample was 600 units long, 60 units wide, and two layers high.

## II. BUCKLING OF FLOWERS

Suppose one has a rectangular sheet of material, described by coordinates  $x$  and  $y$ . Take this rectangular strip and impose a new metric on it so that distances  $dr$  between nearby points originally separated by  $(dx, dy)$  are given by

$$dr^2 = g_{xx}dx^2 + 2g_{xy}dxdy + g_{yy}dy^2. \quad (1)$$

Embed the sheet in three-dimensional space, allowing it to curl as needed to obey this new metric. What shape does it take?

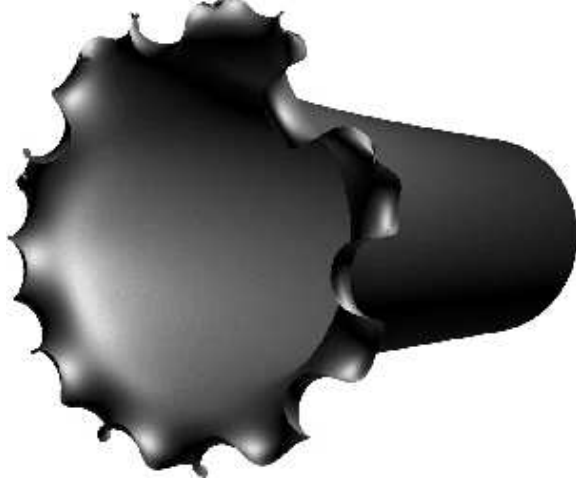


FIG. 2: Result of numerical minimization of Eq. 10 for system twisted around into a cylinder. The  $x$  coordinate of the original material travels in an angular direction around the axis, while the  $y$  coordinate of the original material describes motion along the axis. The metric is  $\sqrt{g_{xx}} = 1/(1+y/2)$ , and the original radius of the cylinder is  $R = 47.8$ . The bound in Eq. 8 is exceeded by a factor of 25. There are around 22 ripples at the edge.

It would be lovely if one could employ differential geometry alone to resolve this question. I have not had success along these lines for the problem depicted in Fig. 1. However, if I digress briefly to discuss flowers rather than leaves, I can make some progress, and want to mention this result before passing on to the main topic of the paper.

Suppose that one adds an additional constraint to the problem, which is that when the sheet is embedded in three dimensions, it is required to be periodic along  $x$ , with period  $2\pi R$ . One has a distorted cylinder, as shown in Fig. 2. One can use results from differential geometry to obtain a simple criterion for when such a structure loses its cylindrical symmetry and buckles. The Gauss–Bonnet theorem[6] applied to this case says that

$$\int ds \kappa = - \int dA K, \quad (2)$$

where  $\kappa$  is the geodesic curvature, and  $K$  is the Gaussian curvature. The first integral is a line integral taken around the edge of the cylinder, while the second is a surface integral.

Continue to use  $x$  and  $y$  to refer to material coordinates. For a metric where only  $g_{xx}(y)$  differs from the value expected in flat space, the Gauss–Codazzi relations[6] give

$$K = -\frac{1}{\sqrt{g_{xx}}} \frac{\partial^2 \sqrt{g_{xx}}}{\partial y^2}. \quad (3)$$

Suppose that after embedding the sheet retains cylindrical symmetry. Then  $\kappa$  is constant. One can place a bound on  $\kappa$ . It cannot be greater in absolute value than  $1/R$ , and it obtains this value only when the edge of the cylinder has splayed out so that the whole outer boundary shares a single tangent plane containing the boundary. Thus the left hand side of Eq. 2 obeys

$$-2\pi \leq \int ds \kappa = 2\pi R\kappa \leq 2\pi \quad (4)$$

Turning now to the right hand side of Eq. 2, one can perform the integral in cylindrical coordinates. At any point indexed by  $y$ , the radius of the cylinder is  $R\sqrt{g_{xx}}$ . Along the  $y$  direction, since  $g_{yy} = 1$ , distances along the sheet are unchanged by introduction

of the metric, and one can write the integral over the Gaussian curvature as

$$\int dA K = \int_0^L dy \int d\theta R \sqrt{g_{xx}(y)} \frac{1}{\sqrt{g_{xx}}} \frac{\partial^2 \sqrt{g_{xx}}}{\partial y^2} \quad (5)$$

$$= 2\pi R \frac{\partial \sqrt{g_{xx}}}{\partial y} \Big|_0^L \quad (6)$$

$$= -2\pi R \frac{\partial \sqrt{g_{xx}(0)}}{\partial y} \quad (7)$$

Returning to Eq. 2, one has the following condition:

$$|R \frac{\partial \sqrt{g_{xx}(0)}}{\partial y}| \leq 1. \quad (8)$$

For metrics with slopes less than this value, it is possible for a cylindrical sheet to maintain cylindrical symmetry, but when the gradient of the metric becomes too steep, a cylindrical sheet must begin to buckle.

Fig 2 provides an example of a buckled cylinder, and the result suggests that the number of ripples at the edge of a cylinder might be given roughly by the quantity on the left hand side of Eq. 8. Because a much more precise wavelength selection rule for leaves is obtained later (Eq. 43), I have not pursued further this possible rule for flowers.

### III. ENERGY OF A THIN SHEET

The energy of a thin sheet is conventionally given by the Föppl–von Kármán equations, and is the sum of two terms, one involving bending of the sheet and the other involving stretching[7, 8]. This starting point is inconvenient for three reasons. First, many formulations employ coordinate systems that are not general enough to encompass the folds and overhangs that occur in this problem. Second, I will deal with sheets that have permanently been stretched, and the equations must be generalized to encompass the deformation. Finally, I need to move easily back and forth between numerical and analytical approaches, and the numerical discretization of the conventional equations is not simple.

I avoid all these problems by starting with a physical model of a sheet based upon a discrete collection of interacting points. I derive the continuum theory from the discrete model rather than by discretizing continuum equations. Similar numerical techniques have been employed frequently in studies of crumpled paper and tethered membranes[9, 10].

Let  $\vec{u}_i$  be a collection of mass points that interact with neighbors, and at rest form a thin flat sheet. Let  $\vec{\Delta}_{ij}$  be equilibrium vector displacements between neighbors  $i$  and  $j$ . When the neighbors are not in equilibrium, the distance between them is  $u_{ij} = |\vec{u}_j - \vec{u}_i|$ . Take the energy corresponding to locations of the mass points to be

$$\mathcal{E} = \frac{\mathcal{K}}{2a} \sum_{\langle ij \rangle} [u_{ij}^2 - \Delta_{ij}^2]^2, \quad (9)$$

where  $\mathcal{K}$  has dimensions of energy per volume,  $a$  has dimensions of length, and the sum is over pairs of neighbors.

With Eq. 9 as a starting point, it is extremely easy to see how to modify equations of elasticity to incorporate a new metric. Write

$$\mathcal{E} = \frac{\mathcal{K}}{2a} \sum_{\langle ij \rangle} [u_{ij}^2 - \sum_{\alpha\beta} \Delta_{ij}^\alpha g_{\alpha\beta} \Delta_{ij}^\beta]^2, \quad (10)$$

where  $g_{\alpha\beta}$  is the metric tensor describing deformations of the sheet. All that has happened, in short, is that the equilibrium distance between material points has changed. My hypothesis is that by specifying different metric tensors  $g$ , often ones with very simple functional forms, one can describe all the buckling cascades we have observed in the laboratory. In particular, since the plastic sheets are torn uniformly in the  $x$  direction, I will assume that the metrics  $g$  are constant in the  $x$  direction, and vary only along  $y$ . Often I will take  $g$  to be diagonal, with  $g_{xx}(y)$  a smoothly varying function and  $g_{yy} = 1$ .

### IV. CONTINUUM LIMIT

The long-wavelength deformations of the points  $\vec{u}_i$  correspond to elastic deformations of a continuous sheet. To form this correspondence, make the replacement

$$\vec{u}_j \approx \vec{u}(\vec{r}_i) + (\vec{\Delta}_{ij} \cdot \vec{\nabla}) \vec{u}(\vec{r}_i), \quad (11)$$

where  $\vec{r}_i$  is the location of  $\vec{u}_i$  in an equilibrium of Eq. 9. Define the strain tensor

$$\epsilon_{\alpha\beta} \equiv \frac{1}{2} \left[ \sum_{\gamma} \frac{\partial u^{\gamma}}{\partial r_{\alpha}} \frac{\partial u^{\gamma}}{\partial r_{\beta}} - g_{\alpha\beta} \right]. \quad (12)$$

This definition reduces to the strain tensor of linear elasticity for small deformations and flat metrics, and generalizes it appropriately when deformations are large and the metric tensor  $g$  differs from the identity. In terms of the strain tensor,  $\mathcal{E}$  can be rewritten as

$$\mathcal{E} = \frac{\mathcal{K}}{a} \sum_i \sum_{j \text{ nbr. of } i} \left[ \sum_{\alpha\beta} \Delta_{ij}^{\alpha} \epsilon_{\alpha\beta}(\vec{r}_i) \Delta_{ij}^{\beta} \right]^2. \quad (13)$$

One has to specify a particular lattice in order to proceed further. If one takes the points  $\vec{u}_i$  to sit on two two-dimensional triangular lattices, stacked over one another as in the first stage of forming an hcp lattice of lattice constant  $a$ , the the energy takes the particular form

$$\mathcal{E} = \frac{\mathcal{K}a^3}{24} \sum_i \left[ \begin{array}{l} 19[\epsilon_{xx} + \epsilon_{yy}]^2 + 38[\epsilon_{xx}^2 + \epsilon_{yy}^2 + 2\epsilon_{xy}^2] \\ + 32\epsilon_{zz}^2 + 16[\epsilon_{yy} + \epsilon_{xx}]\epsilon_{zz} \\ + 32[\epsilon_{yz}^2 + \epsilon_{xz}^2] + 8\sqrt{2}[\epsilon_{yz}(\epsilon_{yy} - \epsilon_{xx}) + 2\epsilon_{xy}\epsilon_{xz}] \end{array} \right] \quad (14)$$

I will employ this continuum functional later as the means to select membrane shapes. Not all terms in it are equally important. However, before arriving at specific deformations to insert into this functional, it is difficult to tell which terms are large and which are small. I therefore begin with a geometrical description of wrinkled sheets, and then return to the question of which shapes minimize energy.

## V. SOLVABLE PROBLEM AT EDGE OF STRIP

The full problem at hand is find the minimum energy state of Eq. 10 or Eq. 14 for a very long strip of finite width and very small thickness  $t$ , subject to a metric  $g_{xx}(y)$  where  $g_{xx}$  has some value  $g_0$  at  $y = 0$  (left hand side of lower panel in Figure 1), and decreases monotonically toward 1 as  $y$  approaches the other side of the strip (right hand side of lower panel in Figure 1). It seems very unlikely that this problem has in general an exact analytical solution. It is not even clear at the outset whether minimum energy states inserted into the functional Eq. 14 should produce the energies proportional to  $t$  that would be characteristic of stretching, or energies proportional to  $t^3$  that would be characteristic of bending.

Therefore, it is useful to find a case where the problem can be solved exactly. The motivation for the solvable problem comes by looking at the lower panel in Figure 1. Imagine making a new infinitely long strip by slicing off the material a short distance  $w$  from the left hand side. If  $w$  is small enough, then the metric  $g_{xx}$  within it should have the form of constant  $g_0$  plus a term linear in  $y$ . If the original length of this strip along the  $x$  direction was  $L$ , now its arc length is  $\sqrt{g_0}L$ . However, in order to be able to join onto the rest of the strip on the right hand side, its total extension in the  $x$  direction must remain  $L$ .

Therefore, I study a thin strip whose metric is

$$\sqrt{g_{xx}(y)} = \sqrt{g_0}(1 - y/R); \quad g_{yy} = 1 \quad (15)$$

where  $R$  is a constant. I look for solutions subject  $\vec{u}(x, y, z)$  subject to the constraint that there be some period  $\lambda$  for which

$$\vec{u}(x + \lambda, y, z) = \hat{x}\lambda + \vec{u}(x, y, z). \quad (16)$$

To obtain the benefits of symmetry, also take

$$y \in [-w/2, w/2] \quad (17)$$

so that the center line of the strip is at  $y = 0$ , rather than one edge.

If a long strip of material is given metric Eq. 15 and no constraint is applied, then the minimum energy configuration is easy to find. The material can relax completely by forming a ring of radius  $R$ , which curls round and round in a circle. Thus one can obtain some intuition about the problem by cutting out the paper figure in Figure 3 and pulling the ends apart horizontally. Let  $\hat{r}_1(\theta)$  and  $\hat{r}_2(\theta)$  be two unit vectors attached to the circular strip, where  $\hat{r}_1$  points around the circumference, and  $\hat{r}_2$  points along the radius. Then the lowest-energy deformations of the paper strip are produced by introducing some bend at every angle  $\theta$  that

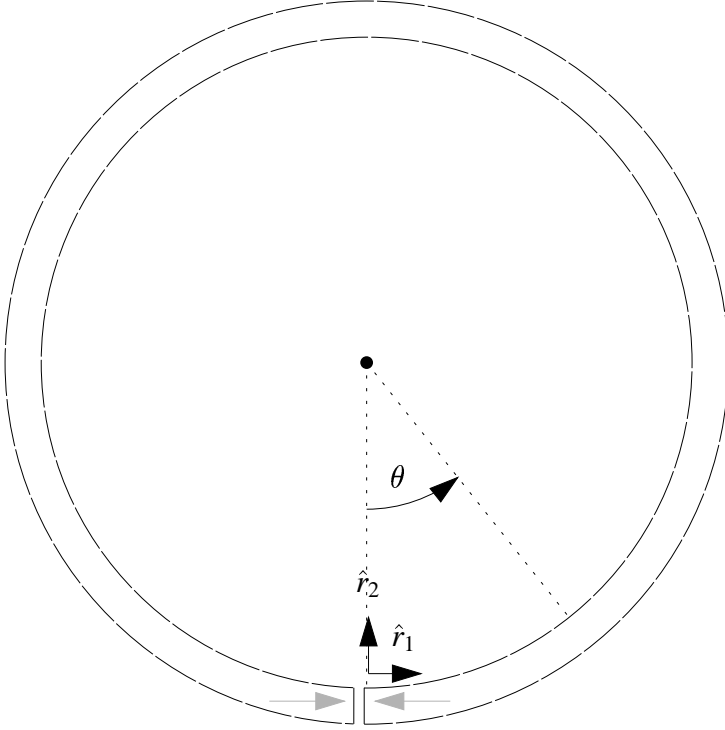


FIG. 3: Cut out this paper figure and place it on a flat surface. Rotate the two ends while pressed flat on the surface so that the two gray arrows point  $180^\circ$  away from one another. Slide the two ends back and forth horizontally in order to see the characteristic shapes that form at the edge of deformed strips.

rotates only around the current direction of  $\hat{r}_2$ . Denote by  $\omega(\theta)$  the rate at which the strip rotates around  $\hat{r}_2$  as a function of the angle  $\theta$ . In a laboratory frame the directions of the unit vectors are determined by

$$\frac{\partial \hat{r}_1}{\partial \theta} = \hat{r}_2 + \omega(\theta) \hat{r}_3 \quad (18a)$$

$$\frac{\partial \hat{r}_2}{\partial \theta} = -\hat{r}_1 \quad (18b)$$

$$\hat{r}_3 = \hat{r}_1 \times \hat{r}_2 \quad (18c)$$

It is easy to check that  $\hat{r}_1$ ,  $\hat{r}_2$ , and  $\hat{r}_3$  remain orthonormal unit vectors under the dynamics described by Eqs. 18. This simple observation leads to the first important conclusion, which is that the constraint in Eq. 16 and the metric in Eq. 15 are incompatible if the strip undergoes bending alone. To show why, relate coordinate  $x$  and angle  $\theta$  through

$$\sqrt{g_0} x = R\theta \quad (19)$$

and note that the location of the center line of the strip is given by

$$\vec{u}(x, 0, 0) \equiv \vec{l}(\theta) \equiv R \int^{\theta} d\theta' \hat{r}_1(\theta'). \quad (20)$$

However, because of Eq. 18b, one can also write

$$\vec{l}(\theta) = -R\hat{r}_2(\theta). \quad (21)$$

Since  $\hat{r}_2$  is a unit vector,  $\vec{l}$  cannot move more than distance  $2R$  from its starting point. Therefore it is impossible to satisfy the constraint in Eq. 16. However, rotations around  $\hat{r}_2$  are the only deformations of the strip that involve nothing but bending, and lead to energies of order thickness  $t^3$ . Thus when the constraint is satisfied, one must expect the energy to include terms of order  $t$ . Although this statement is true, these terms do not dominate the energy in the cases allowing analytical progress. The precise terms of Eq. 14 that dominate will be determined later.

## VI. SOLUTION WITH CONSTANT BENDING

Despite the fact that bending alone cannot solve the physical problem, there is a solution of Eqs. 18 needed for its mathematical development. This solution is found when  $\omega$  is constant. The equations are not obviously solvable, since they are nonlinear, but in fact the exact solution can be expressed in terms of elementary functions. Let

$$\hat{r}_1 = -\operatorname{Re}\left[\frac{i\vec{B}e^{i\theta/\theta_0}}{\theta_0}\right] \quad (22a)$$

$$\hat{r}_2 = \vec{A} + \operatorname{Re}[\vec{B}e^{i\theta/\theta_0}], \quad (22b)$$

where  $\vec{A}$  is real but  $\vec{B}$  is complex. With this choice of  $\hat{r}_1$ , one immediately satisfies 18b. In order for  $\hat{r}_1$  to be a unit vector,

$$\vec{B} \cdot \vec{B} = 0 \quad \text{and} \quad \vec{B} \cdot \vec{B}^* = 2\theta_0^2. \quad (23)$$

Now substitute Eqs. 22 into Eqs. 18c and 18a. They are satisfied if

$$\operatorname{Re}\left[\frac{B}{\theta_0^2}e^{i\theta/\theta_0}\right] = \frac{-i\omega}{4\theta_0} \left[ e^{i\theta/\theta_0} \vec{B} \times \vec{A} - \text{c.c.} + 2\vec{B} \times \vec{B}^* \right] + \vec{A} + \operatorname{Re}[Be^{i\theta/\theta_0}]. \quad (24)$$

Matching up coefficients of different powers of  $\exp[i\theta/\theta_0]$  gives

$$\vec{A} = \frac{i\omega}{2\theta_0} \vec{B} \times \vec{B}^* \quad (25a)$$

$$\vec{B}(\theta_0^{-2} - 1) = \frac{-i\omega}{2\theta_0} \vec{B} \times \vec{A}. \quad (25b)$$

Substituting Eq. 25a into Eq. 25b and using Eq. 23 gives

$$\theta_0^2 = \frac{1}{\omega^2 + 1}. \quad (26)$$

Choosing any  $\vec{B}$  that satisfies Eq. 23, one therefore has solution, where  $\vec{A}$  is determined by Eq. 25a. In particular, when  $\hat{r}_1(0) = \hat{x}$  and  $\hat{r}_2(0) = \hat{y}$ , one has explicitly

$$\hat{r}_1 = \cos(\theta/\theta_0)\hat{x} + \theta_0 \sin(\theta/\theta_0)\hat{y} + \theta_0 \omega \sin(\theta/\theta_0)\hat{z} \quad (27a)$$

$$\hat{r}_2 = -\theta_0 \sin(\theta/\theta_0)\hat{x} + (1 - \theta_0^2(1 - \cos(\theta/\theta_0)))\hat{y} - \omega \theta_0^2(1 - \cos(\theta/\theta_0))\hat{z} \quad (27b)$$

$$\hat{r}_3 = -\theta_0 \omega \sin(\theta/\theta_0)\hat{x} - \theta_0^2 \omega [1 - \cos(\theta/\theta_0)]\hat{y} + (\theta_0^2 + [1 - \theta_0^2]\cos(\theta/\theta_0))\hat{z}. \quad (27c)$$

and

$$l^x = R \sin(\theta/\theta_0) \theta_0 \quad (28a)$$

$$l^y = R(1 - \cos(\theta/\theta_0))\theta_0^2 \quad (28b)$$

$$l^z = R\omega(1 - \cos(\theta/\theta_0))\theta_0^2 \quad (28c)$$

## VII. SOLUTION WITH CONSTANT BENDING AND TORSION

Since bending around  $\hat{r}_2$  is not a general enough deformation of the strip to satisfy constraint Eq. 16, it seems intuitively clear that the next-lowest set of strip deformations can be produced by allowing torsion; that is, bends around  $\hat{r}_1$ . Let  $\dot{\phi}$  describe the rate at which twisting around  $\hat{r}_2$  occurs, and let  $\dot{\psi}$  describe the rate at which twisting around  $\hat{r}_1$  occurs. A first case allowing exact solution is when  $\dot{\phi}$  and  $\dot{\psi}$  are constant. Then Eqs. 18 become

$$\frac{\partial \hat{r}_1}{\partial \theta} = \dot{\phi} \hat{r}_1 \times \hat{r}_2 + \hat{r}_2 \quad (29a)$$

$$\frac{\partial \hat{r}_2}{\partial \theta} = \dot{\psi} \hat{r}_1 \times \hat{r}_2 - \hat{r}_1. \quad (29b)$$

Define

$$\begin{pmatrix} \hat{s}_1 \\ \hat{s}_2 \end{pmatrix} = \frac{1}{\omega} \begin{pmatrix} \dot{\phi} & \dot{\psi} \\ -\dot{\psi} & \dot{\phi} \end{pmatrix} \begin{pmatrix} \hat{r}_1 \\ \hat{r}_2 \end{pmatrix} \quad (30)$$

where

$$\omega = \sqrt{\dot{\phi}^2 + \dot{\psi}^2} \quad (31)$$

Rewriting Eqs. 29 in terms of these new variables, they become

$$\frac{\partial \hat{s}_1}{\partial \theta} = \hat{s}_2 + \omega \hat{s}_1 \times \hat{s}_2 \quad (32a)$$

$$\frac{\partial \hat{s}_2}{\partial \theta} = -\hat{s}_1. \quad (32b)$$

Eqs. 18 and Eqs. 32 are identical, except that the latter involve  $s$  instead of  $r$ . Therefore, choosing a coordinate system where  $\hat{x}'$  points along  $\hat{s}_1(0)$  and  $\hat{y}'$  points along  $s_2(0)$ , the  $\hat{x}'$ ,  $\hat{y}'$  and  $\hat{z}'$  coordinates of  $\hat{s}_1$  and  $\hat{s}_2$  are given once again by Eqs. 27.

### VIII. SOLUTION WITH OSCILLATING BENDING AND TORSION

This solution still does not solve the physical problem at hand, because the strip twists endlessly around the original  $\hat{x}$  axis. In order to avoid twisting the strip, the torsion  $\psi$  must oscillate between positive and negative values. A solution of this type can be found by taking

$$\dot{\phi} = \omega \cos \alpha \theta \quad (33a)$$

$$\dot{\psi} = \omega \sin \alpha \theta \quad (33b)$$

Now the equations describing rotations of the strip unit vectors are nonlinear and have non-constant coefficients. However, they can still be solved. Once again, define a new coordinate system with Eq. 30. Substituting Eqs. 33b into Eqs. 18 gives now

$$\frac{\partial \hat{s}_1}{\partial \theta} = \hat{s}_2(1 + \alpha) + \omega \hat{s}_1 \times \hat{s}_2 \quad (34a)$$

$$\frac{\partial \hat{s}_2}{\partial \theta} = -\hat{s}_1(1 + \alpha). \quad (34b)$$

Defining

$$\theta' = (1 + \alpha)\theta, \quad \omega' = \omega/(1 + \alpha) \quad \text{and} \quad \theta_0'^2 = \frac{1}{1 + \omega'^2} \quad (35)$$

one again recovers Eqs. 18, and its solution Eqs. 27 in terms of primed variables. That is,

$$\hat{s}_1 = \cos(\theta/\theta_0')\hat{x} + \theta_0' \sin(\theta/\theta_0')\hat{y} + \theta_0' \omega \sin(\theta/\theta_0')\hat{z} \quad (36a)$$

$$\hat{s}_2 = -\theta_0' \sin\left(\frac{\theta}{\theta_0'}\right)\hat{x} + (1 - \theta_0'^2(1 - \cos(\frac{\theta}{\theta_0'})))\hat{y} - \omega' \theta_0'^2(1 - \cos(\frac{\theta}{\theta_0'}))\hat{z} \quad (36b)$$

$$\hat{s}_3 = -\theta_0' \omega' \sin\left(\frac{\theta}{\theta_0'}\right)\hat{x} - \theta_0'^2 \omega' [1 - \cos(\frac{\theta}{\theta_0'})]\hat{y} + (\theta_0'^2 + [1 - \theta_0'^2] \cos(\frac{\theta}{\theta_0'}))\hat{z}. \quad (36c)$$

Finally the solutions can correspond to the shapes at the edge of wrinkled sheets. To see when they are physically acceptable, one has to invert all the linear transforms and write the expression for  $\hat{r}_1$  explicitly. It is

$$\hat{r}_1^x = \cos \alpha \theta \cos(\theta'/\theta_0') + \theta_0' \sin \alpha \theta \sin(\theta'/\theta_0') \quad (37a)$$

$$\hat{r}_1^y = \theta_0' \cos \alpha \theta \sin(\theta'/\theta_0') - \sin \alpha \theta (1 - \theta_0'^2(1 - \cos \theta'/\theta_0')) \quad (37b)$$

$$\hat{r}_1^z = \theta_0' \omega' \cos \alpha \theta \sin(\theta'/\theta_0') + \omega' \theta_0'^2 \sin \alpha \theta (1 - \cos(\theta'/\theta_0')) \quad (37c)$$

To satisfy the constraint Eq. 16, when one integrates  $\hat{r}_1$  to get  $\vec{l}$ , the  $x$  component must increase indefinitely, while the  $y$  and  $z$  components must oscillate. The solution acts this way if and only if

$$\alpha \theta = \pm \theta'/\theta_0' \quad (38)$$

The two signs in Eq. 38 produce identical solutions, as Eq. 37 is invariant under  $\theta'_0 \rightarrow -\theta'_0$ . Adopting the minus sign, one has

$$\alpha = -\frac{(1 + \omega^2)}{2} \quad (39)$$

$$\Rightarrow \theta'_0 = \frac{1 - \omega^2}{1 + \omega^2} \quad (40)$$

The wavelength of the pattern is given by the angle through which  $\theta$  travels so that the smallest nonzero Fourier component of the pattern goes through one period, meaning that  $\theta$  travels through  $2\pi/\alpha$ . One now finds that the wavelength of the pattern  $\lambda = l(2\pi/\alpha)$  is

$$\lambda = \frac{2\pi}{|\alpha|} R(1 - \theta'_0)/2 = \frac{4\pi R \omega^2}{(1 + \omega^2)^2}. \quad (41)$$

Since the strip travels an arclength  $2\pi R/\alpha$  when  $\theta$  goes through  $2\pi/\alpha$ , one can find the constant part of the metric,

$$\sqrt{g_0} = 1 + 1/\omega^2 \Rightarrow \omega = \frac{1}{\sqrt{\sqrt{g_0} - 1}}. \quad (42)$$

Furthermore, using Eq. 15, one can determine the wavelength  $\lambda$  from

$$\frac{2\pi}{\lambda} = \frac{g_0}{2R(\sqrt{g_0} - 1)} = \frac{1}{4(\sqrt{g_0} - 1)} \left| \frac{\partial g_{xx}}{\partial y} \right|_{y=0}. \quad (43)$$

Since  $\omega$  and  $R$ , or equivalently  $\lambda$ , are the only parameters describing the solution, it has been determined completely by  $\sqrt{g_0}$  and the slope of the metric. What Eq. 43 means is that if one has a strip originally of length  $L \gg R$ , then imposes the metric Eq. 15, grabs the two ends and puts them at some horizontal distance  $L/\sqrt{g_0} < L$ , then the sheet will ripple, and the wavelength of the ripple will uniquely be given by Eq. 43.

Some images of solutions appear in Fig. 4. The radius  $R$  is adjusted in each case so that the wavelength  $\lambda$  remains constant. Drawing a number of such pictures, one finds that there is an upper limit of  $\sqrt{g_0} \approx 5.61$  for solutions of this type. When  $\sqrt{g_0}$  is larger than this value, the solution collides with itself in the center of the wave and becomes self-intersecting.

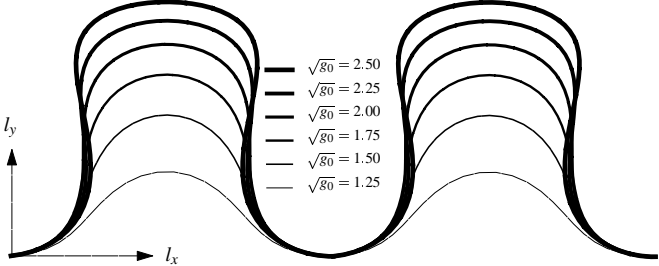


FIG. 4: Height of edge  $l^y(\theta)$  versus length of edge  $l^x(\theta)$  for solution given in Eq. 37 and various values of  $\sqrt{g_0}$ .

## IX. IMPLICATIONS FOR ENERGY FUNCTIONAL

Assuming that displacements are of the form given in Eq. 37, it is possible to return to the functional Eq. 14 and decide which terms dominate the energy of a stretched sheet. From the customary theory of thin sheets one expects the energy come from the sum of two terms. The first term is the stretching energy of the sheet, and is of order  $t$ , where  $t$  is the thickness of the sheet; in Eq. 14, the stretching energy would arise from the terms on the top of the right hand side that involve no derivatives with respect to  $z$ . The second term is the bending energy of the sheet, and it is proportional to  $t^3$ .

This expectation is correct. Bending and stretching energies dominate the energy functional. Which of them dominates is a subtle matter. The stretching energy is proportional to the thickness of the sheet  $t$  while the bending energy is proportional to the thickness of the sheet cubed,  $t^3$ . In the limit of thin sheets, one would think that the stretching energy would be dominant. However, matters are not that simple, because the energy is proportional to the width of the strip  $w$  to the fifth power,  $w^5$ . The limit I believe is most interesting in practice is

$$\left( \frac{w}{R} \right)^2 \ll \frac{t}{R} \ll \frac{w}{R}. \quad (44)$$

In this limit the bending energy proportional to  $t^2/R^2$  dominates the energy, while the stretching energy, proportional to  $w^4/R^4$ , can be neglected.

To obtain the energy formally, take  $\vec{u}$  in the form

$$\vec{u}(x, y, z) = \vec{l}(\theta) + \hat{r}_2 y + (\hat{r}_3 - q(\theta, y) \hat{r}_1) z, \quad (45)$$

with  $\theta$  related to  $x$  by Eq. 19. Then

$$\frac{\partial \vec{u}}{\partial x} = \frac{\sqrt{g_0}}{R} \frac{\partial}{\partial \theta} \left[ \vec{l}(\theta) + \hat{r}_2 y + (\hat{r}_3 - q \hat{r}_1) z \right] \quad (46a)$$

$$= \sqrt{g_0} \left[ \hat{r}_1 + \frac{y}{R} \frac{\partial \hat{r}_2}{\partial \theta} + \frac{z}{R} \left( \frac{\partial \hat{r}_3}{\partial \theta} - q \frac{\partial \hat{r}_1}{\partial \theta} \right) - \frac{\partial q}{\partial \theta} \hat{r}_1 \frac{z}{R} \right] \quad (46b)$$

$$= \sqrt{g_0} \left[ \hat{r}_1 \left( 1 - \frac{y}{R} - \left[ \dot{\phi} + \frac{\partial q}{\partial \theta} \frac{z}{R} \right] \right) + \frac{z}{R} (q - \dot{\psi}) \hat{r}_2 + \left[ \frac{y}{R} \dot{\psi} - \frac{z}{R} \dot{\phi} q \right] \hat{r}_3 \right] \quad (46c)$$

$$\frac{\partial \vec{u}}{\partial y} = \hat{r}_2 - z \frac{\partial q}{\partial y} \hat{r}_1 \quad (46d)$$

$$\frac{\partial \vec{u}}{\partial z} = \hat{r}_3 - q \hat{r}_1. \quad (46e)$$

The form of the displacement in Eq. 45 would be particularly simple if the function  $q(\theta, y)$  were not present. When  $q(\theta, y) = 0$ , the displacements in Eq. 45 are those that are appropriate for the simple torsion of a beam. The energy is dominated by a term proportional to  $\epsilon_{xz}^2$ , and turns out also to be proportional to the moment of inertia of the strip around the  $\hat{R}_1$  axis. It is not energetically favorable for a thin sheet to shear in this way. The energy is greatly reduced by eliminating shear in the  $xz$  plane, and accepting instead a small amount of compression along  $x$ . The function  $q(\theta, y)$  allows the sheet to distort in this way.

Since Eq. 45 was introduced with no justification, it is sensible to wonder whether there is not a variant on this form for  $\vec{u}$  that would lead to much lower energies. Apart from the fact that repeated attempts to vary Eq. 45 in some way did not lead to a significant lowering of the energy, the most persuasive argument is probably that energies resulting from this form are a few percent lower than direct numerical minimization of Eq. 10, under conditions that will be described a bit later.

To proceed, compute the strain tensor from Eqs. 12. The metric tensor is diagonal, and its  $xx$  component is given by Eq. 15. The computation is straightforward, but the expressions have many terms, and it does not seem worthwhile recording all of them here. The one term that does need to be recorded is

$$\epsilon_{xz} = \sqrt{g_0} \left[ \frac{y(\dot{\psi} - q) - qR}{2R} \right]. \quad (47a)$$

From Eq. 44 observe that  $y/R \leq w/(2R)$  is a small quantity. All terms of first order in  $w/R$  can be made to vanish by taking

$$q(\theta, y) = \frac{\dot{\psi}(\theta)y}{R}. \quad (48)$$

With this choice of  $q$ , the displacements  $\vec{u}$  are completely specified.

Inserting the expressions for  $\epsilon_{\alpha\beta}$  into Eq. 10, one has the following results. Since there are only two layers in the  $z$  direction, carry out that sum explicitly, but convert sums in the  $x$  and  $y$  direction to integrals, using the fact that the area per particle is  $\sqrt{3/4a^2}$ . The leading term proportional to the sheet thickness is

$$\mathcal{K} \frac{aLw^5}{R^4} \frac{1}{L} \int_0^L dx \frac{(57g_0^2 + 16g_0 + 32)\dot{\psi}^4 + 32g_0\dot{\psi}^2}{1920\sqrt{3}}, \quad (49)$$

but the term that dominates the energy when inequalities Eq. 44 hold is

$$\mathcal{K} \frac{at^2Lw}{R^2} \frac{1}{L} \int_0^L dx \frac{(76g_0\dot{\psi}^2 + 57g_0^2\dot{\phi}^2)\sqrt{3}}{72}. \quad (50)$$

When Eq. 50 dominates the energy, the strip is wide enough so that  $w \gg t$ , but not so wide that it is favorable to begin buckling or forming fine structure in the  $y$  direction.

The various powers of  $g_0$  appearing in Eq. 50 are somewhat unexpected. They arise because the microscopic lattice underlying the calculation has been stretched, and its elastic properties made anisotropic by the new metric. The calculations are producing a specific description for how stretching material in the  $x$  direction by a factor of  $\sqrt{g_0}$  changes its elastic properties. This

description is unlikely to apply to the polymeric materials in which most experiments are conducted. For this reason, direct numerical studies of the bending of strips have been carried out in such a way that  $g_0$  in Eq. 50 should be set to 1. Rather than starting with a strip of length  $L = \lambda$ , stretching it to length  $\lambda\sqrt{g_0}$ , and then introducing a gradient in the metric along  $y$ , the numerical studies start with a strip of length  $L$ , introduce a linear gradient of slope  $1/R$  in the metric along  $y$ , and then constrain the ends of the strip to sit at distance  $\lambda = L/\sqrt{g_0}$ . That is, the constraint at the ends of the strip instead of Eq. 16 is

$$\vec{u}(x+L, y, z) = \hat{x}\lambda + \vec{u}(x, y, z). \quad (51)$$

The energy of a strip prepared in this way is

$$\mathcal{K} \frac{at^2 L w}{R^2} \frac{1}{L} \int_0^L dx \frac{(76\dot{\psi}^2 + 57\dot{\phi}^2) \sqrt{3}}{72}. \quad (52)$$

## X. EXACT SOLUTION OF ELASTIC PROBLEM

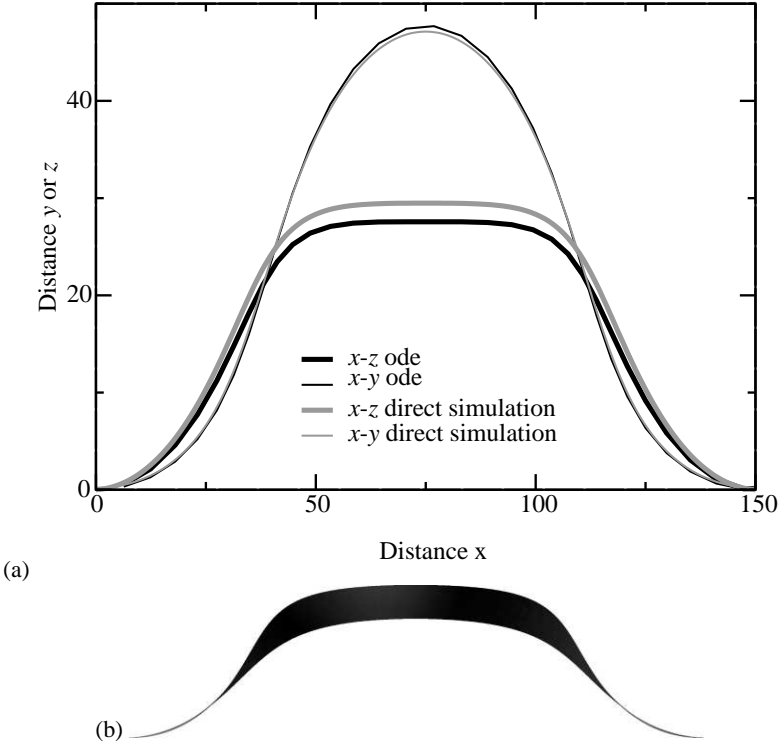


FIG. 5: (a) Comparison of the shape given by Eq. 37 with the result of a direct numerical minimization of Eq. 10, for a strip 201 atoms long in the  $x$  direction, and 12 layers wide in the  $y$  direction, constrained to have horizontal period of 150 so that  $\sqrt{g_0} = 4/3$ , and  $R = 63.7$ , using Eq. 43. The energy predicted by the complete function Eq. 14 with  $L = 200$ ,  $w = 9.1$ , is  $1.55\mathcal{K}a^3$ . The energy predicted by Eq. 52 is  $1.43\mathcal{K}a^3$ . The energy found numerically is  $1.37\mathcal{K}a^3$ . The slight discrepancy between predicted and actual shape and energy appear due to a slight additional buckling at the edges of the strip beyond what is predicted by Eq. 45. (b) Three-dimensional visualization of the final shape resulting from the numerical minimization.

The solution of Eq. 37 was obtained by assuming that  $\dot{\phi}$  and  $\dot{\psi}$  have the forms given in Eq. 33b. These choices for the torsion and bending of the strip did make it possible to find a shape for the strip that was consistent with the constraint in Eq. 16, and with a few other physical considerations.

It is natural to suspect that varying  $\dot{\phi}$  and  $\dot{\psi}$  away from the arbitrary forms obtained by guessing would lead to additional solutions, some most likely of lower energy. This is not the case. The solution obtained here turns out to be exact.

A first indication that the solution is exact comes from a direct numerical minimization of Eq. 10, the result of which is given in Figure 5 for a numerical strip of size  $201 \times 12 \times 2$ . The numerical value of the energy obtained in the minimization is 9% lower than the value calculated in Eq. 52. To check whether this discrepancy is a finite-size effect, or whether there are some

leading contributions to the energy still missing from the energy, I performed an additional numerical minimization on a system of size  $401 \times 15 \times 2$ . The shape of the solution is now indistinguishable from the analytical prediction. The way to scale the energy so that it becomes independent of system size is  $\mathcal{E}L/w$ . According to the analytical calculations, this quantity should equal 29.4. For the system of length 201, the numerics give 26.3, while for the system of length 401 the numerics give 27.3. The results are plausibly converging to the expected value, but because of the length of time needed for the numerical minimizations, the matter was not pursued further.

At first I tried to prove that Eq. 37 minimizes Eq. 10, subject to the constraint in Eq. 16. After failing to find a correct demonstration, I realized that the situation is different than I had supposed. It is not possible to find small variations of the functions  $\psi$  and  $\phi$  that preserve the constraint. With any small change in the bending and torsion, the strip does not return to its original orientation when  $x = L$ . This conclusion is counter-intuitive. If one actually builds the strip in Fig. 3, then it is easy to grab the strip at two ends and deform it slightly in the middle, making it appear that small deformations of  $\phi$  and  $\psi$  preserving the constraint ought to exist. The mathematical analysis does not agree. Probably the deformations of the strip one performs with the hands also involve slight changes in its overall length, a possibility that is not allowed by Eq. 45. Thus the solutions found here are general enough to include the ground state of Eq. 10, but not to include all of the low-energy deviations from the ground state.

The results concerning the constraint are as follows: Suppose one has slight perturbations of  $\dot{\phi} + \delta\dot{\phi}$  and  $\dot{\psi} + \delta\dot{\psi}$ , and that to linear order, the unit vectors  $\vec{r}$  change to

$$\hat{r}_i \rightarrow \hat{r}_i + \vec{\epsilon}_i. \quad (53)$$

To preserve the orthonormality of the unit vectors,

$$\hat{r}_i \cdot \epsilon_i = 0 \quad \text{and} \quad \hat{r}_1 \cdot \vec{\epsilon}_2 + \hat{r}_2 \cdot \vec{\epsilon}_1 = 0. \quad (54)$$

Let

$$\vec{\epsilon}_1 = \epsilon_1^2 \hat{r}_2 + \epsilon_1^3 \hat{r}_3 \quad (55a)$$

$$\vec{\epsilon}_2 = \epsilon_1^1 \hat{r}_1 + \epsilon_2^3 \hat{r}_3. \quad (55b)$$

Superscripts here denote indices, not exponents. Then one finds to linear order that

$$\begin{pmatrix} \dot{\epsilon}_2^1 \\ \dot{\epsilon}_2^3 \\ \dot{\epsilon}_1^3 \end{pmatrix} = \begin{pmatrix} 0 & \dot{\phi} & -\dot{\psi} \\ -\dot{\phi} & 0 & -1 \\ \dot{\psi} & 1 & 0 \end{pmatrix} \begin{pmatrix} \epsilon_2^1 \\ \epsilon_2^3 \\ \epsilon_1^3 \end{pmatrix} + \begin{pmatrix} 0 \\ \delta\dot{\psi} \\ \delta\dot{\phi} \end{pmatrix}, \quad (56)$$

with  $\dot{\phi}$  and  $\dot{\psi}$  given by Eq. 33b. Define the matrix

$$\mathcal{M}(\theta) = \begin{pmatrix} 0 & \omega \cos \alpha \theta & -\omega \sin \alpha \theta \\ -\omega \cos \alpha \theta & 0 & -1 \\ \omega \sin \alpha \theta & 1 & 0 \end{pmatrix} \quad (57)$$

Then

$$\begin{pmatrix} \epsilon_2^1 \\ \epsilon_2^3 \\ \epsilon_1^3 \end{pmatrix} = \int_0^\theta d\theta' \exp[\mathcal{N}(\theta, \theta')] \begin{pmatrix} 0 \\ \delta\dot{\psi}(\theta') \\ \delta\dot{\phi}(\theta') \end{pmatrix}, \quad (58)$$

where

$$\mathcal{N}(\theta, \theta') = \int_{\theta'}^\theta d\theta'' \mathcal{M}(\theta''). \quad (59)$$

In particular,

$$\mathcal{O}(\theta') = \mathcal{N}(2\pi/\alpha, \theta') \quad (60)$$

$$= \begin{pmatrix} 0 & -(\omega/\alpha) \sin \alpha \theta' & -(\omega/\alpha)(1 - \cos \alpha \theta') \\ (\omega/\alpha) \sin \alpha \theta' & 0 & -(2\pi/\alpha - \theta') \\ (\omega/\alpha)(1 - \cos \alpha \theta') & (2\pi/\alpha - \theta') & 0 \end{pmatrix} \quad (61)$$

For all values of  $\theta' < 2\pi/\alpha$ ,  $\mathcal{O}(\theta')$  has three orthogonal eigenvectors, and the eigenvalues are

$$\lambda = 0 \quad \text{and} \quad \lambda_{\pm} = \pm i\sqrt{(2\pi/\alpha - \theta')^2 + (\omega/\alpha)^2 \sin^2 \theta' \alpha + (\omega/\alpha)^2 [1 - \cos \theta' \alpha]^2} \quad (62)$$

The question of imposing the constraint in Eq. 16 now becomes whether there exist any functions  $\delta\dot{\phi}$  and  $\delta\dot{\psi}$  such that

$$\begin{pmatrix} 0 \\ 0 \\ 0 \end{pmatrix} = \int_0^{2\pi/\alpha} d\theta' \exp[\mathcal{O}(\theta')] \begin{pmatrix} 0 \\ \delta\dot{\psi}(\theta') \\ \delta\dot{\phi}(\theta') \end{pmatrix}. \quad (63)$$

If so, they constitute nonzero minima of the functional

$$\mathcal{R} = \frac{\int_0^{2\pi/\alpha} d\theta'' \int_0^{2\pi/\alpha} d\theta' \begin{pmatrix} 0 \\ \delta\dot{\psi}(\theta'') \\ \delta\dot{\phi}(\theta'') \end{pmatrix}^\dagger \exp[\mathcal{O}^\dagger(\theta'')] \exp[\mathcal{O}(\theta')] \begin{pmatrix} 0 \\ \delta\dot{\psi}(\theta') \\ \delta\dot{\phi}(\theta') \end{pmatrix}}{\int_0^{2\pi/\alpha} d\theta' [\delta\dot{\psi}(\theta')]^2 + [\delta\dot{\phi}(\theta')]^2} \quad (64)$$

The functional is easier to understand if one introduces a new function  $\delta\dot{\chi}$ , that would have to turn out to be zero, and minimizes

$$\mathcal{R} = \frac{\int_0^{2\pi/\alpha} d\theta'' \int_0^{2\pi/\alpha} d\theta' \begin{pmatrix} \delta\dot{\chi}(\theta'') \\ \delta\dot{\psi}(\theta'') \\ \delta\dot{\phi}(\theta'') \end{pmatrix}^\dagger \exp[\mathcal{O}^\dagger(\theta'')] \exp[\mathcal{O}(\theta')] \begin{pmatrix} \delta\dot{\chi}(\theta') \\ \delta\dot{\psi}(\theta') \\ \delta\dot{\phi}(\theta') \end{pmatrix}}{\int_0^{2\pi/\alpha} d\theta' [\delta\dot{\psi}(\theta')]^2 + [\delta\dot{\phi}(\theta')]^2 + [\delta\dot{\chi}(\theta')]^2} \quad (65)$$

Taking three functional derivatives of  $\mathcal{R}$  with respect to the three unknown functions gives

$$\exp[-\mathcal{O}(\theta)] \int_0^{2\pi/\alpha} d\theta' \exp[\mathcal{O}(\theta')] \begin{pmatrix} \delta\dot{\chi}(\theta') \\ \delta\dot{\psi}(\theta') \\ \delta\dot{\phi}(\theta') \end{pmatrix} = \mathcal{R} \begin{pmatrix} \delta\dot{\chi}(\theta) \\ \delta\dot{\psi}(\theta) \\ \delta\dot{\phi}(\theta) \end{pmatrix} \quad (66)$$

Thus the only extremum is for

$$\begin{pmatrix} \delta\dot{\chi}(\theta) \\ \delta\dot{\psi}(\theta) \\ \delta\dot{\phi}(\theta) \end{pmatrix} = \frac{1}{\mathcal{R}} \exp[-\mathcal{O}(\theta)] \vec{p}, \quad (67)$$

with

$$\vec{p} = \int_0^{2\pi/\alpha} d\theta' \exp[\mathcal{O}(\theta')] \begin{pmatrix} \delta\dot{\chi}(\theta') \\ \delta\dot{\psi}(\theta') \\ \delta\dot{\phi}(\theta') \end{pmatrix} \quad (68)$$

$$\Rightarrow \vec{p} = \frac{2\pi}{\alpha \mathcal{R}} \vec{p} \Rightarrow \mathcal{R} = \frac{2\pi}{\alpha} \quad (69)$$

Since  $\mathcal{R} > 0$ , it is impossible to perturb the bending and torsion away from Eq. 33b and preserve the constraint.

This calculation does not completely clarify matters. The extremum is a maximum, not a minimum. It is not hard to find functions that make  $\mathcal{R}$  as small as desired, although none of them make  $\mathcal{R}$  vanish. A sequence of functions approaching delta functions makes  $\mathcal{R}$  small. This sequence converges pointwise to zero and is of no interest.

## XI. COMPOSITE SOLUTIONS

Based upon exact results for a strip one can construct sensible estimates for properties of a buckling cascade. Suppose one returns to Eq. 37, and instead of setting  $\alpha$  to the value in Eq. 38 that allows the sheet to extend indefinitely in the  $x$  direction sets it instead to some other value? Then the solution wiggles, but in the end returns to its starting point. Rewrite  $\hat{r}_1^x$  as

$$\hat{r}_1^x = \frac{1}{2}(1 - \theta'_0) \cos\left(\frac{\theta(1 + \alpha)}{\theta'_0} + \alpha\theta\right) + \frac{1}{2}(1 + \theta'_0) \cos\left(\frac{\theta(1 + \alpha)}{\theta'_0} - \alpha\theta\right) \quad (70)$$

If  $\alpha$  does not differ too much from its value in Eq. 38, then the period of the first cosine is much larger than the period of the second. Upon integrating to find  $\vec{l}(\theta)$ , one finds that the solution constitutes a circle with a wiggling edge whose overall large radius is

$$R^{(2)} = \frac{f}{\gamma}, \quad (71)$$

where

$$\gamma \equiv (1 + \alpha)/\theta'_0 + \alpha = \alpha + \sqrt{(1 + \alpha)^2 + \omega^2}. \quad (72)$$

and

$$f \equiv \frac{1 - \theta'_0}{2} \quad (73)$$

The wavelength of the short-wavelength wiggle is approximately

$$\lambda^{(1)} = \frac{2\pi f R}{(1 + \alpha)/\theta'_0 - \alpha}, \quad (74)$$

since this is roughly the integral of  $r_1^x$  over the period of the fast wiggle.

To traverse the large circle,  $\theta$  travels through an angle  $2\pi/\gamma$ , involving an arc length of  $\sqrt{g_0}2\pi R/\gamma$ . However, the apparent arc length of the circle is  $2\pi R^{(2)}$ . Thus the original strip problem can be mapped onto a new one, where the total length of the new strip is given by

$$L^{(2)} = fL \quad (75)$$

or equivalently

$$\sqrt{g_0^{(2)}} = f\sqrt{g_0}. \quad (76)$$

Because  $\omega$  and  $\alpha$  can be varied independently, one can vary  $R^{(2)}$  and  $g_0^{(2)}$  independently. However, there are limits to the variation. For example, according to Eq. 35,  $-1 < \theta'_0 < 1$  (depending on the sign of the square root), so  $\sqrt{g_0^{(2)}}$  is always less than  $\sqrt{g_0}$ .

This new effective circle can itself curl up into an extended pattern, whose wavelength, according to Eq. 43 is

$$\lambda^{(2)} = \frac{4\pi R^{(2)}(\sqrt{g_0^{(2)}} - 1)}{g_0^{(2)}} \quad (77)$$

and where the amplitude of the wiggle is given by

$$\omega^{(2)} = \frac{1}{\sqrt{f\sqrt{g_0} - 1}}, \quad (78)$$

as in Eq. 42.

One can now ask whether or not it is energetically favorable for a strip with a linear gradient to form a composite structure with more than one wavelength. Using  $f$  and  $\gamma$  as independent variables, one finds that

$$\omega = (\gamma + 1) \sqrt{\frac{f}{1 - f}}. \quad (79)$$

Returning to Eq. 52 when  $\dot{\phi}$  and  $\dot{\psi}$  are described by Eq. 33b one has that

$$\mathcal{E} = \frac{\mathcal{K}aL^2w}{R^2} \frac{\omega^2}{2} \frac{(76 + 57)\sqrt{3}}{72}. \quad (80)$$

Suppose that the energy of a strip with two generations of waves is given by the sum of Eq. 80 for the first generation, and the same expression but with  $L$ ,  $R$ , and  $\omega$  replaced by  $L^{(2)}$ ,  $R^{(2)}$ , and  $\omega^{(2)}$  respectively. The resulting energy is proportional to

$$\mathcal{E}_{\text{composite}} \propto \frac{(\gamma + 1)^2 f}{1 - f} + \frac{1}{f\sqrt{g_0} - 1} \frac{\gamma^2}{f}. \quad (81)$$

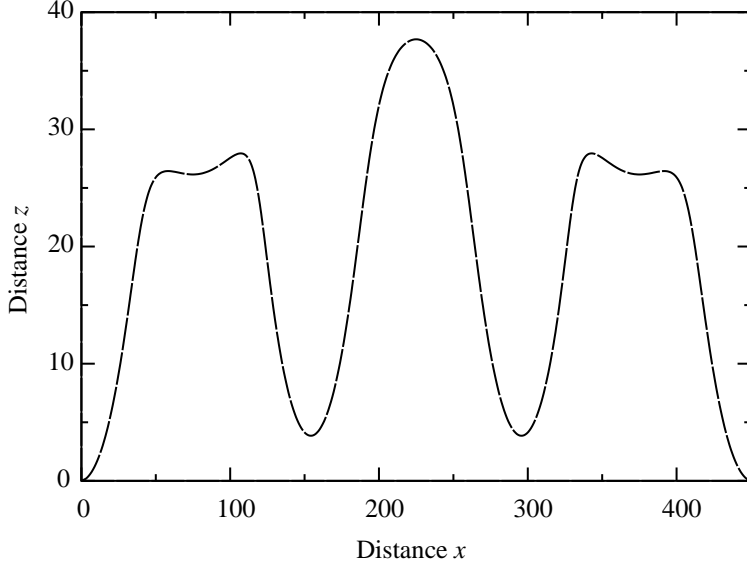


FIG. 6: Numerical minimization of the same system described in Fig. 5, but with  $\lambda$  and  $L$  three times as long. The total energy is  $4.08\mathcal{K}a^3$ , which is less than the value  $3 \times 1.37\mathcal{K}a^3$  one would obtain simply by pasting together three copies of Fig. 5. The fact that the wavelength of the long structure is three times the wavelength of the shorter one is in accord with theoretical predictions, but is also heavily influenced by the boundary conditions.

The minimum of this energy is given by solving a cubic equation for  $f$ . This equation has two complex roots, and one real root that is always less than one, but with the property that  $f\sqrt{g_0} > 1$ . Thus the solution is physically sensible, and the calculation predicts that for sufficiently long strips it is always favorable to develop more than one wavelength.

The precise predictions for the long and short wavelengths cannot be taken too seriously because the approximation that the total energy is the sum of energies of waves at the two different scales is not likely to be very good. Furthermore, the long and short wavelengths are not predicted to be very different from one another, as shown in Table I. They differ by a factor of around 2.

$\sqrt{g_0}$	$\lambda^{(1)}/R$	$\lambda^{(2)}/R$
1.5	1.50	3.35
2.0	1.88	4.21
2.5	2.01	4.36
3.0	2.05	4.27
3.5	2.05	4.10
4.0	2.04	3.90
4.5	2.02	3.70
5.0	1.57	3.52

TABLE I: Approximate wavelengths of short and long oscillations in strip as a function of metric constant  $\sqrt{g_0}$ .

I have obtained some direct numerical confirmation that this prediction is correct. Returning to the numerical setting of Fig. 5, I triple the length of the system, fix the boundaries at distance  $3\lambda$ , leave all else as before, and minimize the energy Eq. 10. The strip develops a composite structure in which the long wavelength is 3 times the short wavelength, and with an energy that is somewhat less than 3 times the energy of the structure 1/3 as long.

It is plausible that the lowest-energy state for the simple metric in Eq. 15 involves a cascade of oscillations on many scales, but I have not yet obtained detailed evidence. Many other problems remain to be addressed, including the application of the ideas obtained here to the more complex metrics illustrated in Fig. 1.

### Acknowledgments

Eran Sharon discussed these problems with me for weeks, and spent months carrying out experiments, before I finally began to see there was something interesting to be done. Thanks to Ralf Stephan for pointing out Ref. [5]. Financial support from the National Science Foundation (DMR-9877044 DMR-0101030) is gratefully acknowledged.

---

1. E. Sharon, B. Roman, M. Marder, G. Y. Shin, and H. L. Swinney, *Nature* (2002), in press.
2. M. Byrne, M. Timmermans, C. Kidner, and R. Martinssen, *Current Opinion in Plant Biology* **4**(1), 38 (2001).
3. P. B. Green, *American Journal of Botany* **86**, 1059 (1999).
4. P. Green, C. Steele, and S. C. Rennich, *Annals of Botany* **77**, 515 (1996).
5. S. Nechaev and R. Voituriez, *Journal of Physics A* **34**, 11069 (2001).
6. A. V. Pogorelov, *Differential Geometry* (P Noordhoff N. V., Groningen, 1956).
7. L. D. Landau and E. M. Lifshitz, *Theory of Elasticity* (Pergamon Press, Oxford, 1986), 3rd ed.
8. E. H. Mansfield, *The Bending and Stretching of Plates* (Pergamon, New York, 1964).
9. H. S. Seung and D. R. Nelson, *Physical Review A* **38**, 1005 (1988).
10. A. E. Lobkovsky and T. A. Witten, *Physical Review E* **55**, 1577 (1997).